CARBON 50 (2012) 2581–2587

Available at www.sciencedirect.com
SciVerse ScienceDirect
journal homepage: www.elsevier.com/locate/carbon

Restoration of graphene from graphene oxide by defect repair

Meng Cheng, Rong Yang, Lianchang Zhang, Zhiwen Shi, Wei Yang, Duoming Wang, Guibai Xie, Dongxia Shi, Guangyu Zhang *

Beijing National Laboratory for Condensed Matter Physics, Chinese Academy of Sciences, Beijing 100190, China

A R T I C L E I N F O

Article history:
Received 10 November 2011
Accepted 5 February 2012
Available online 14 February 2012

A B S T R A C T

A simple and efficient method to repair defects in graphene oxide (GO) is reported, accompanied by a simultaneous reduction process by a methane plasma. The graphene after repair is of high quality. For a typical monolayer after repair and reduction, the minimum sheet resistance at the Dirac point and the Raman D/G peak intensity ratio are about 9.0 kΩ/□ and ~0.53, respectively.

1. Introduction

Graphene is a two-dimension carbon with unique mechanical, chemical, and electronic properties [1–7]. Reduction of GO for graphene has attracted considerable attention for its massive output and low-cost [8–10]. Many approaches have been developed, including thermal annealing [8,11–16], chemical [17–21], photocatalytic [22,23] and plasma reduction [7,24], and it turns out to be efficient. However, abundant defects are still existed after reduction, which are introduced by the oxidation and exfoliation process. These defects can degrade graphene's quality much, i.e., electrical conductivity and mechanical stiffness, thus are not favorable. It is demonstrated that defect repair could improve the conductivity of restored GO film, rather than only with reduction [13,25–27]. However, this repaired and reduced graphene still show strong intensity of the Raman D peak, indicating the existence of dense defects [14,26]. Moreover, the defect repair mechanism is still not clear. Here we report a methane plasma restoration approach, by which defects of GO can be repaired efficiently, accompanied with a simultaneous reduction process. The repair occurs at the edges of defects (or holes), and eventually restore the GO into high quality graphene. The resulting graphene have the lowest D peak and highest conductivity ever reported for GO derived graphene.

2. Experimental

2.1. *Samples preparation*

In this work, GO colloidal suspensions were prepared from purely natural graphite by Hummer's method [28]. Before we spin-coated GO suspension on Si/SiO_2 substrate (P type heavy doping Si with 300-nm-thick thermal SiO_2), the substrate was soaked in 3-amino-propyltriethoxysilane for about 20 min. For the electrical measurement, three terminal devices were fabricated for as-made GO and repaired GO (r-GO), assisted by electron beam lithography, metal deposition by electron beam evaporation, and lifting-off technique.

2.2. *Defect repair for graphene basal plane*

Highly oriented pyrolytic graphite (HOPG, A-grade, from Advanced Ceramics) substrates with fresh cleaved surfaces were first etched by O_2-plasma at ~90 °C with plasma power of 120 W for around 30 s to introduce dense dot defects in the topmost layer. In order to view these defects directly, we enlarged them into small pits with size of 10–20 nm with hydrogen (H_2) plasma at ~525 °C with plasma power of 100 W for 10 min, while etching occurs only at the edges around the defects [29]. The defect repair was carried out in a remote plasma enhanced chemical vapor deposition system at ~560 °C

* *Corresponding author*: Fax: +86 10 6255 6598.
E-mail address: gyzhang@iphy.ac.cn (G. Zhang).
0008-6223
doi:10.1016/j.carbon.2012.02.016

using pure methane (CH_4) as the precursor. The gas pressure and radio frequency plasma power were 0.20 Torr and 100 W, respectively.

2.3. Defect repair for graphene oxide

With the same approach to repair HOPG we can also restore GO to high-quality graphene, but at a slightly higher temperature of ~575 °C. Contrast to the lately reported method in which artificially introduced defects of HOPG were partly repaired by acetylene with Fe as catalyst [30], our repair method would obtain a high degree of restoration without catalyst.

2.4. Characterization

The topography information was acquired by atomic force microscope (AFM, MultiMode IIId, Veeco Instruments Inc.). Raman spectroscopy was carried out using a Horiba Jobin Yvon LabRAM HR-800 Raman microscope ($\lambda = 532$ nm). Elemental composition analysis was carried out using X-ray photoelectron spectroscopy (XPS, ESCALAB 250, Thermo Fisher Scientific Inc.) using focused monochromatized Al Kα radiation. Electrical measurements were using Agilent semiconductor parameter analyzer (4156C) under high vacuum in a four-probe station system.

3. Results and discussion

3.1. Demonstration of defect repair with graphene basal plane

Prior to repairing GO, we carried out defect repair for graphene basal plane with artificially introduced defects to demonstrate the capability of repair by methane plasma. AFM was used to view HOPG surface before and after healing for the same area (Fig. 1a and b). From the images we can directly see that most of the pits on the HOPG surface created by O_2 and H_2 plasma etching were filled out to reform the smooth surface after healing. This process was also supported by the Raman measurements, since the D peak (D, for defect mode) nearly disappeared after healing (Fig. 1c). A schematic drawing of the repairing process of these artificial defects created in the graphene basal plane is shown in Fig. 1d. Some pits in Fig. 1b are not fully filled but can be removed by extended healing. It was noted that the depositing process started from the edges instead of on the bottom of pits or the intact HOPG surface, revealing the importance of edges in restoring structure of graphene. This kind of extended growth at the graphene edges was consistent with what we observed previously for nanographene growth [31].

3.2. Structure and elemental composition analysis

To investigate the restoration process, we carried out defect repair for GO with different restoring durations. The corresponding AFM images and the Raman spectra are shown in Fig. 2a–d. Fig. 2a shows a typical as-made monolayer GO sheet deposited on Si/SiO_2 substrate. Most of the GO are monolayer sheets with heights in the range of 1–2 nm and lateral dimensions of few microns (Fig. 2a). Compared with the pristine graphene with a thickness of ~0.8 nm [5], the higher thickness of as-made GO is due to the presence of the covalent C–O bonds at both top and bottom surfaces, distorted sp^3 carbon lattices and absorbed contaminations [19,32]. After methane plasma treatment for 3 min, all organic contaminations adsorbed on both GO and substrate were removed, thus a clean and smooth surface was achieved and the thickness became lower (Fig. 2b). As the duration increased, the r-GO became thinner and smoother due to reduction of oxygen functional groups and sp^3 carbon domains. Meanwhile, all defects or holes in GO were getting repaired (Fig. 2c and d). It was noted that nanographene started to nucleate on the surface of the r-GO when the duration of methane plasma treatment was over 10 min (Fig. S1).

The Raman spectra of the as-made and plasma treated samples is shown in Fig. 3a, and the corresponding D/G (G for graphite mode) intensity ratios (I_D/I_G) are plotted in Fig. 3b. The I_D/I_G decreases after the restoration process from 1.03 for as-made GO to 0.53 for 10-min treated samples, and it is far below those of other restored GO ever reported [11,13,24]. Since I_D/I_G is proportional to the average size of the sp^2 carbon domain, the decreased I_D/I_G is attributed to the removal of defects and the conversion of sp^3 to sp^2 carbons [33,34]. The XPS result also supports the high efficiency of the reduction process. Resolution C1s peak of as made GO reveal that its oxygen functional groups mainly consist of C–O (hydroxyl and epoxy, ~286.4 eV), C=O (carbonyl, ~288.2 eV) (Fig. 3c) [20,35]. After a 10 min repair with methane plasma, these two peaks decrease obviously and C–C peak becomes dominating, indicating that most of the oxygen functional groups are removed (Fig. 3d). Based on these results, our r-GO is more close to pristine graphene in terms of structure than those of reduced GO without defect repair.

3.3. Control experiments

In order to further understand the defect repair efficiency of this methane plasma treatment, we carried out reduction of as-made GO in H_2 atmosphere at high temperature of ~800 °C for a comparison. H_2 annealing can cause C–O bonds breaking and edge-passivation in GO [14,36]. The Raman spectrum of these reduced samples shows very high D peak (Fig. 4), indicating abundant structural defects in presence. We also treated these reduced GO afterwards with methane plasma to repair the defects. However, we found the repair was less efficient for H_2-reduced GO than it for as-made GO under the same repair conditions, as revealed in the Raman data in Fig. 4. Moreover, we used H_2 plasma to reduce the as-made GO at a temperature of ~750 °C. We found that GO, after H_2 plasma reduction, became rougher and porous (Fig. S2a). Although the quality of reduced GO by H_2 plasma was poor, the disordered edges were trimmed to some extent [37], thus a slightly drop of intensity of the D peak was observed in the Raman spectra (Fig. S2b). Additionally, transport measurements of these samples show a nonlinear I–V dependence and very low electrical conductivity (Fig. S2c). These control experiments revealed the indispensability of carbon in restoration process.

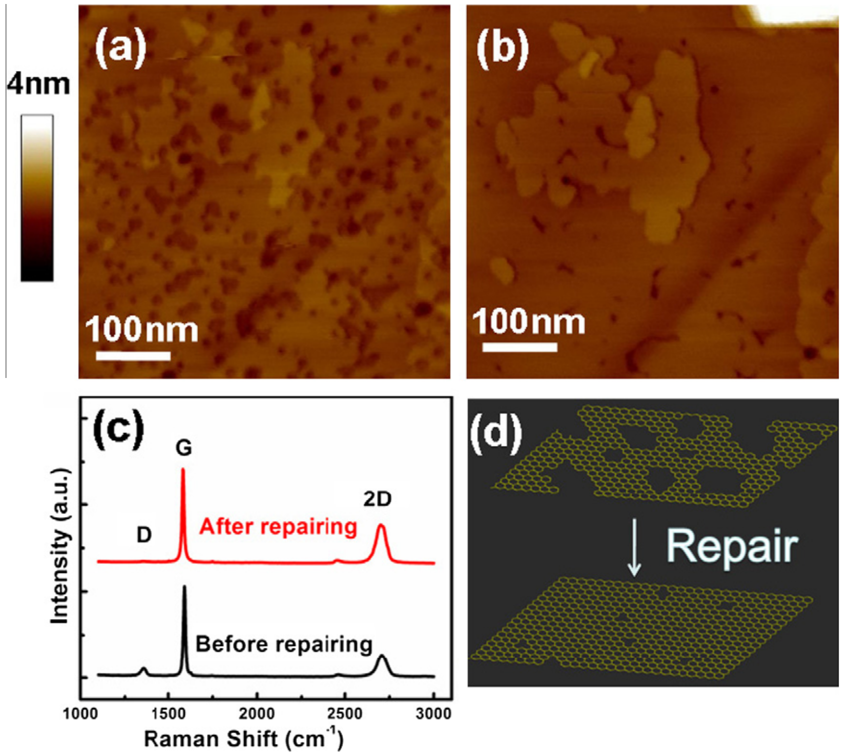

Fig. 1 – Defect repair on HOPG surface. (a) AFM image of HOPG surface with artificial defects created by O_2 plasma etching at room temperature and followed by H_2 plasma etching at ~525 °C to form monolayer pits. (b) AFM image of the area in (a) after repairing defects. (c) The Raman spectra of HOPG surface before and after repair. (d) Schematic drawing of the repair process.

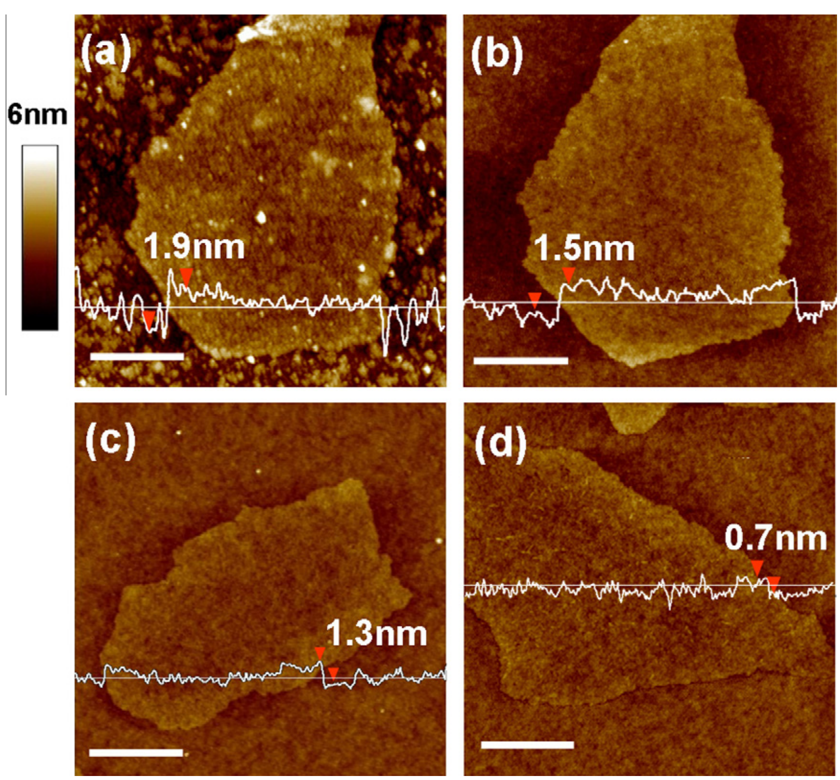

Fig. 2 – AFM characterization of GO and r-GO (a) AFM images of as-made graphene oxide. (b)–(d) Graphene sheets with different repair durations of 3, 6 and 10 min, respectively (b) is the same area with (a). The inserted white curves are AFM height profiles with each height value labeled and scale bar is 500 nm.

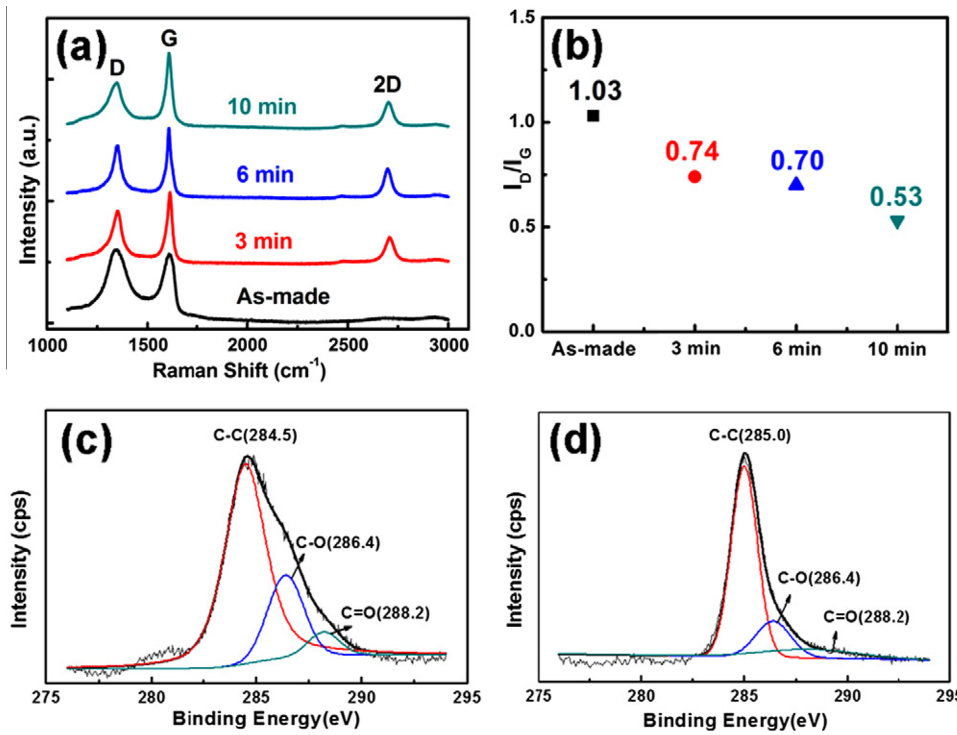

Fig. 3 – Raman spectra and XPS spectra of GO and r-GO. (a) Raman spectra and corresponding D/G intensity ratios (b) of as-made GO and samples with different repair durations of 3, 6 and 10 min. The C1s XPS spectra of as made GO (c) and r-GO after 10-min repair (d).

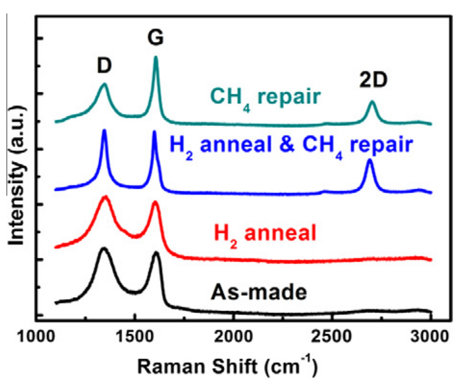

Fig. 4 – Raman spectra of GO with different treatments. As-made GO (black), H_2 annealed GO (red), H_2 annealed and then repaired by CH_4 (blue) and directly CH_4 repairing for 10 min (Green). (For interpretation of the references to colour in this figure legend, the reader is referred to the web version of this article.)

3.4. *Electrical measurements*

We also carried out electrical measurements for r-GO, as electrical conductivity is a direct criterion for judging the quality of r-GO. The schematic and a typical AFM image of the device are shown in Fig. 5a. The conductivity of the r-GO is found to be over 4 orders of magnitude higher than that of as-made GO. For a typical device (shown in Fig. 5a), the sheet resistance R_S ($R_S = RW/L$, where R is the maximum resistance of the device at the Dirac point; W and L are the graphene width and channel length, respectively) is about 9.0 kΩ/□, which is close to pristine graphene [37,38]. This achieved graphene device also gives a very high conductivity σ around 1590 S/cm (calculated with $\sigma = 1/R_S{\cdot}t$, where t is the film thickness, about 0.7 nm of this r-GO sheet). After an *in situ* vacuum annealing to remove the absorbed impurities [34], the Dirac point of the r-GO device shows a positive shift of about 30 V in contrast to as made GO (Fig. 5b). The p-type behavior for the r-GO devices, which has been reported for other reduced GO, is also observed in our low temperature measurements and can be explained by presence of persistent positively charged impurities and substrate charge transfer [25]. The non-linear I–V characteristic at high bias is also observed for these r-GO devices (Fig. 5b inset) [39]. The output characteristic is showed in Fig. 5c, as expected for a typical graphene based field-effect transistor [9]. We also measured the R_S for many other devices, and all of them showed good conductivity with R_S below 20 kΩ/□. Note that the contact resistance was not eliminated from the above calculations; the actual R_S for these r-GO devices were even lower.

Temperature dependent electrical measurements were carried out in vacuum from room temperature down to ~4 K. The superior conduction performance of our r-GO is also supported by its high conductivity even at that low temperature with only a slightly rise in resistance upon cooling down (Fig. 5d) [14]. Compared with pristine graphene, r-GO has a larger sheet resistance due to its corrugated surface and residual defects and its electrical conductance can be described by the 2-D variable range hopping model [25,39]. The

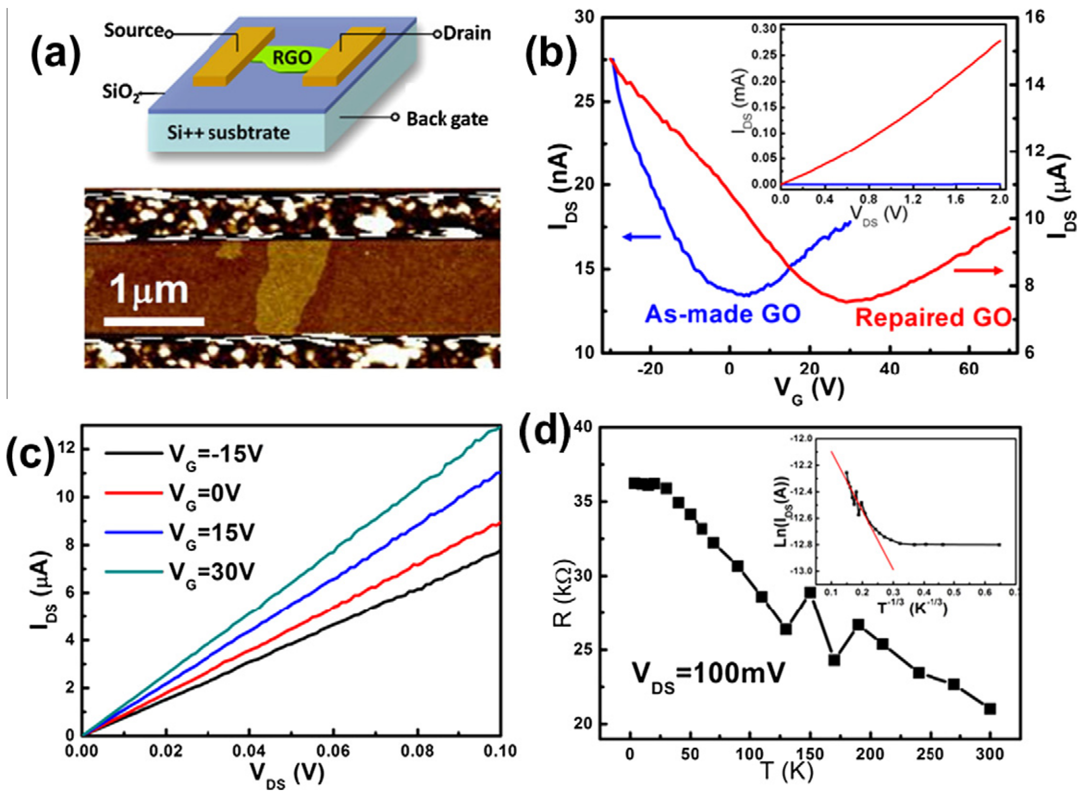

Fig. 5 – Electrical properties of r-GO sheet. (a) Schematic diagram (top) and a typical AFM image (down) of a r-GO sheet device. (b) I–V G curves for as-made GO (blue) and repaired GO (red) (Vbias = 0.1 V), whose I–V curves are showed in inset diagram respectively. (c) I–V curves for different gate voltages that shows the tunability of graphene-based material and linear relation of I–V. (d) Resistance at different temperate of a repaired GO device. Inset is a plot of current against $T^{-1/3}$ whose partly linearly fit is showed as the red line. (For interpretation of the references to colour in this figure legend, the reader is referred to the web version of this article.)

conductance (G) vs. Temperature (T) relation could be expressed as:

$$G(T) = G_1 \exp\left(-\frac{B}{T^{1/3}}\right) + G_0 \tag{1}$$

where B is the hopping parameter, defined as:

$$B = \left(\frac{3}{kN(E_F)L_l^2}\right)^{1/3} \tag{2}$$

where k_B is Boltzmann's constant, $N(E_F)$ is the density of mobile carriers and L_l is the localization length. In this relation, the first term becomes dominant at relatively higher temperature, thus the plots of $\ln(I_{DS})$ vs. $T^{-1/3}$ can be fitted linearly in the left regime (red line in Fig. 5d inset), where the slope could be estimated by B. Compared with other reported results of reduced GO [7,25,39], our r-GO exhibits remarkably lower slope, indicating its higher quality, since lower slope indicates ether larger $N(E_F)$ or L_l, which should be attributed to enlargement of graphene crystallite domains.

Through the comparison of R_S of pristine graphene prepared through mechanical cleavage and those GO derived graphene reported elsewhere (Fig. 6), our restoration approach has better performance in recovering of high electrical property. Note that, the reported results of Dai et al. (CH_4/H_2, at 1000 °C, σ of 350–410 S/cm) [27], Liang et al. (C_2H_2/H_2, at

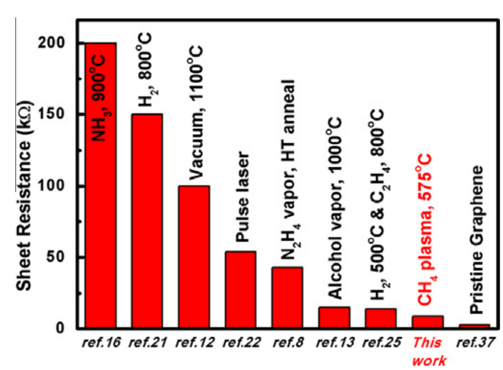

Fig. 6 – Comparison of sheet resistances from previous methods, ours and pristine graphene. Number in square bracket is the corresponding reference.

1000 °C, σ of 1425 S/cm) [26], Su et al. (alcohol, at 1000 °C) [13] and López et al. (C_2H_4, at 800 °C) [25] have already achieved good conductive behavior by defect repair with thermal annealing in certain carbonaceous gas. However, our method requires lower temperature (<600 °C) and shorter time (10 min is enough), and get higher conductivity (1590 S/cm) or lower sheet resistance (9.0 kΩ/□) (see Fig. 6). Our method provides the facile and fast way for GO repairing.

4. Conclusion

We developed an efficient approach for restoring high-quality graphene from GO by defect repair. Oxygen groups in GO are largely removed and defects are successfully repaired during this fast and simple restoring approach. The obtained materials have regained the superior properties in both structure and electrical conductivity. The repair method provides a potential way for scaled-up and low-cost graphene production.

Acknowledgements

This work was supported by the 100 Talents Program of the Chinese Academy of Sciences (CAS), the National Science Foundation of China (NSFC) (Grant Nos. 10974226, 11074288, and 11174333) and National 973 project of China (Grant Nos. 2010CB934202 and 2012CB921302).

Appendix A. Supplementary data

Supplementary data associated with this article can be found, in the online version, at doi:10.1016/j.carbon.2012.02.016.

REFERENCES

[1] Huang X, Qi X, Boey F, Zhang H. Graphene-based composites. Chem Soc Rev 2012;41:666–86.
[2] Huang X, Yin ZY, Wu SX, Qi XY, He QY, Zhang QC, et al. Graphene-based materials: synthesis, characterization, properties, and applications. Small 2011;7(14):1876–902.
[3] Jiang HJ. Chemical preparation of graphene-based nanomaterials and their applications in chemical and biological sensors. Small 2011;7(17):2413–27.
[4] Geim AK, Novoselov KS. The rise of graphene. Nat Mater 2007;6(3):183–91.
[5] Novoselov KS, Geim AK, Morozov SV, Jiang D, Zhang Y, Dubonos SV, et al. Electric field effect in atomically thin carbon films. Science 2004;306(5296):666–9.
[6] Novoselov KS, Jiang D, Schedin F, Booth TJ, Khotkevich VV, Morozov SV, et al. Two-dimensional atomic crystals. Proc Natl Acad Sci U S A 2005;102(30):10451–3.
[7] Gomez-Navarro C, Weitz RT, Bittner AM, Scolari M, Mews A, Burghard M, et al. Electronic transport properties of individual chemically reduced graphene oxide sheets. Nano Lett 2007;7(11):3499–503.
[8] Eda G, Fanchini G, Chhowalla M. Large-area ultrathin films of reduced graphene oxide as a transparent and flexible electronic material. Nat Nanotechnol 2008;3(5):270–4.
[9] Tung VC, Allen MJ, Yang Y, Kaner RB. High-throughput solution processing of large-scale graphene. Nat Nanotechnol 2009;4(1):25–9.
[10] Li D, Muller MB, Gilje S, Kaner RB, Wallace GG. Processable aqueous dispersions of graphene nanosheets. Nat Nanotechnol 2008;3(2):101–5.
[11] Chen WF, Yan LF. Preparation of graphene by a low-temperature thermal reduction at atmosphere pressure. Nanoscale 2010;2(4):559–63.
[12] Wu JB, Becerril HA, Bao ZN, Liu ZF, Chen YS, Peumans P. Organic solar cells with solution-processed graphene transparent electrodes. Appl Phys Lett 2008;92(26):263302–4.
[13] Su CY, Xu YP, Zhang WJ, Zhao JW, Liu AP, Tang XH, et al. Highly efficient restoration of graphitic structure in graphene oxide using alcohol vapors. ACS Nano 2010;4(9):5285–92.
[14] Li XL, Zhang GY, Bai XD, Sun XM, Wang XR, Wang E, et al. Highly conducting graphene sheets and Langmuir–Blodgett films. Nat Nanotechnol 2008;3(9):538–42.
[15] Wei ZQ, Wang DB, Kim S, Kim SY, Hu YK, Yakes MK, et al. Nanoscale tunable reduction of graphene oxide for graphene electronics. Science 2010;328(5984):1373–6.
[16] Li XL, Wang HL, Robinson JT, Sanchez H, Diankov G, Dai HJ. Simultaneous nitrogen doping and reduction of graphene oxide. J Am Chem Soc 2009;131(43):15939–44.
[17] Moon IK, Lee J, Ruoff RS, Lee H. Reduced graphene oxide by chemical graphitization. Nat Commun 2010;1:73–9.
[18] Chen WF, Yan LF, Bangal PR. Chemical reduction of graphene oxide to graphene by sulfur-containing compounds. J Phys Chem C 2010;114(47):19885–90.
[19] Stankovich S, Dikin DA, Piner RD, Kohlhaas KA, Kleinhammes A, Jia Y, et al. Synthesis of graphene-based nanosheets via chemical reduction of exfoliated graphite oxide. Carbon 2007;45(7):1558–65.
[20] Pei SF, Zhao JP, Du JH, Ren WC, Cheng HM. Direct reduction of graphene oxide films into highly conductive and flexible graphene films by hydrohalic acids. Carbon 2010;48(15):4466–74.
[21] Dai HJ, Li XL, Zhang GY, Bai XD, Sun XM, Wang XR, et al. Highly conducting graphene sheets and Langmuir–Blodgett films. Nat Nanotechnol 2008;3(9):538–42.
[22] Huang L, Liu Y, Ji LC, Xie YQ, Wang T, Shi WZ. Pulsed laser assisted reduction of graphene oxide. Carbon 2011;49(7):2431–6.
[23] Williams G, Seger B, Kamat PV. TiO_2-graphene nanocomposites. UV-assisted photocatalytic reduction of graphene oxide. ACS Nano 2008;2(7):1487–91.
[24] Baraket M, Walton SG, Wei Z, Lock EH, Robinson JT, Sheehan P. Reduction of graphene oxide by electron beam generated plasmas produced in methane/argon mixtures. Carbon 2010;48(12):3382–90.
[25] Lopez V, Sundaram RS, Gomez-Navarro C, Olea D, Burghard M, Gomez-Herrero J, et al. Chemical vapor deposition repair of graphene oxide: a route to highly conductive graphene monolayers. Adv Mater 2009;21(46):4683–6.
[26] Liang YY, Frisch J, Zhi LJ, Norouzi-Arasi H, Feng XL, Rabe JP, et al. Transparent, highly conductive graphene electrodes from acetylene-assisted thermolysis of graphite oxide sheets and nanographene molecules. Nanotechnology 2009;20(43):434007–13.
[27] Dai BY, Fu L, Liao L, Liu N, Yan K, Chen YS, et al. High-quality single-layer graphene via reparative reduction of graphene oxide. Nano Res 2011;4(5):434–9.
[28] Hummers WS, Offeman RE. Preparation of graphitic oxide. J Am Chem Soc 1958;80(6):1339.
[29] Yang R, Zhang LC, Wang Y, Shi ZW, Shi DX, Gao HJ, et al. An anisotropic etching effect in the graphene basal plane. Adv Mater 2010;22(36):4014–9.
[30] Kholmanov IN, Edgeworth J, Cavaliere E, Gavioli L, Magnuson C, Ruoff RS. Healing of structural defects in the topmost layer of graphite by chemical vapor deposition. Adv Mater 2011;23(14):1675–8.
[31] Zhang LC, Shi ZW, Wang Y, Yang R, Shi DX, Zhang GY. Catalyst-free growth of nanographene films on various substrates. Nano Res 2011;4(3):315–21.
[32] Mkhoyan KA, Contryman AW, Silcox J, Stewart DA, Eda G, Mattevi C, et al. Atomic and electronic structure of graphene-oxide. Nano Lett 2009;9(3):1058–63.
[33] Tuinstra F, Koenig JL. Raman spectrum of graphite. J Chem Phys 1970;53(3):1126–30.

[34] Wang HL, Robinson JT, Li XL, Dai HJ. Solvothermal reduction of chemically exfoliated graphene sheets. J Am Chem Soc 2009;131(29):9910–1.
[35] Stankovich S, Piner RD, Nguyen ST, Ruoff RS. Synthesis and exfoliation of isocyanate-treated graphene oxide nanoplatelets. Carbon 2006;44(15):3342–7.
[36] Kobayashi Y, Fukui K, Enoki T, Kusakabe K, Kaburagi Y. Observation of zigzag and armchair edges of graphite using scanning tunneling microscopy and spectroscopy. Phys Rev B 2005;71(19):193406–10.
[37] Shi Z, Yang R, Zhang L, Wang Y, Liu D, Shi D, et al. Patterning graphene with zigzag edges by self-aligned anisotropic etching. Adv Mater 2011;23(27):3061–5.
[38] Reina A, Jia XT, Ho J, Nezich D, Son HB, Bulovic V, et al. Large area, few-layer graphene films on arbitrary substrates by chemical vapor deposition. Nano Lett 2009;9(1):30–5.
[39] Kaiser AB, Gomez-Navarro C, Sundaram RS, Burghard M, Kern K. Electrical conduction mechanism in chemically derived graphene monolayers. Nano Lett 2009;9(5):1787–92.